Int. J. Heat Mass Transfer. Vol. 27, No. 9, pp. 1473–1483, 1984
Printed in Great Britain

0017–9310/84 $3.00 + 0.00
© 1984 Pergamon Press Ltd.

Effect of thoracic and abdominal pressure waves on blood flow in cardiopulmonary resuscitation

R. BEYAR, E. KIMMEL, S. SIDEMAN, U. DINNAR and Y. KISHON

The Julius Silver Institute of Biomedical Engineering, and the Department of Chemical Engineering, Technion-Israel Institute of Technology, Haifa 32000, Israel

(*Received* 7 *February* 1984)

Abstract—Based on the assumption that externally induced pressure variations inside the chest cavity generate life saving blood flow during cardiopulmonary resuscitation (CPR) in cardiac arrest, mathematical models of increased complexities were developed to describe the flow phenomena in the cardiovascular system. The lumped parameter representation of the cardiovascular system describes the flow phenomena during CPR, and is used to optimize the present CPR technique as well as to suggest a new CPR procedure. Clinical experimental studies (dogs) confirm the prediction that a sequential phased abdomino-thoracic compression (PCCPR) yields blood flows which are twice the values obtained in the classical CPR mode of manual chest compression. The newly suggested PCCPR technique greatly improves vital organs' blood flow in CPR and opens a new direction in the field of emergency medicine.

INTRODUCTION

THE PRIMARY goal of the cardiopulmonary resuscitation (CPR) is to affect systemic blood flow through the body organs, so as to prevent the anoxic death of vital organs in case of cardiac arrest. Indeed, the universally used CPR technique, which is based on intermittent compressions of the chest by an external force, interposed with forced ventilation, is associated with systemic blood flow generation [1]. The mechanism affecting the blood flow during CPR is commonly attributed to the compression of the heart between the thoracic spine and the sternum [2, 3]. However, this classical hypothesis is questionable in view of the following new evidence:

(a) Vigorous cough causes blood flow during cardiac arrest, both in man and in a dog model [4].

(b) Both the aortic and the mitral valves (Fig. 1) are open during the compression of the heart, thus indicating that the left heart is serving as a passive conduit rather than an active pump [5].

(c) Ventilation during chest compression augments the systemic blood flow [6].

The above observations, which suggest that the blood flow in CPR is due to intrathoracic pressure variation, has stimulated the development of a new CPR technique which is based on the simultaneous ventilation and chest compression (SVCCPR) [7–10]. Indeed, the intrathoracic pressure, as well as the cardiac output and carotid flow, are significantly increased by this technique. The systemic blood flow in SVCCPR increases even more when the intrathoracic pressure is increased by binding the abdominal cavity with external straps [11–13].

Of particular interest to CPR physiology is the understanding of the blood flow distribution during CPR. The body control mechanisms, as well as the local metabolic effects, modify the system parameters and control the blood flow distribution to the various organs during CPR. This is evident by injecting radioactive microspheres into the blood stream and monitoring their distribution in the various body organs during CPR [14, 15]. The results indicate that while the perfusion of all the organs (total systemic flow) is only 10–30% of its baseline normal value, the ratio of blood flow in the brain to the flow in the heart and kidney is greater during CPR than during normal conditions. A different approach to augment blood flow to the vital organs was tried by Weisfeldt *et al.* [16], who used high doses of adrenaline, which significantly increases the peripheral resistance, thus directing the blood to flow to the vital organs.

A CPR technique which increases the general, or regional, blood flow to the vital organs and improves the chances of survival and recovery from cardiac arrest is thus highly desired. The quest for an efficient CPR procedure has recently led to the development of the phased compression CPR (PCCPR) technique which employs interposing abdominal compressions between thoracic compressions and actually doubles the cardiac output and the blood flow to the cranium [17]. Voorhees *et al.* [18] have obtained similar effects by sequential compressions of the thorax and the abdomen.

The present report deals with the analysis of the hemodynamic phenomena during CPR, based on a computer simulation of CPR and clinical *in vivo* studies with dogs. The analysis is based on a systematic study of the effects of the intrathoracic and intra-abdominal pressure variation on the hemodynamics during cardiac arrest (CPR) [19–22] under various operating conditions. The study thus offers a better understanding of the mechanism of the blood flow in the various modes of CPR. Not least important, the study demonstrates the application of mathematical

NOMENCLATURE

C	capacitance	R_{st}	resistance of collapsed conduit, equation (4)
L	inductance	R_0	resistance of the uncollapsed–collapsible segment
P	pressure	Q	flow.
P_{ab}	intra-abdominal pressure		
P_{th}	intrathoracic pressure		
R	resistance		

modeling as a tool for the exploration and development of an optimal new CPR technique for the treatment of cardiac arrest and, perhaps, a cardiac assist device for the treatment of cardiogenic shock.

MODELING OF BLOOD CIRCULATION DURING CPR

A variety of mathematical approaches has been used to describe the cardiovascular system [23, 24] which is schematically depicted in Fig. 1. The models range from simple approaches, which describe the arterial system as a Windkessel model [25], to highly detailed compartmental ones [26]. The constitutive equations of each of the system compartments can be based on pulsatile flow in elastic arteries, on a transmission line model [27] or a simple electrical RLC analog [23, 26]. Here, we adopt the latter approach whereby the flow network is made of arterial segments which are characterized by a resistance R, inductance L, and capacitance C. The pressure P and the flow rate Q are analogous to the voltage and current, respectively, in the electrical circuit.

With reference to Fig. 2, the pressure and the flow rate in an arterial segment i are interrelated by

$$\frac{dQ_i}{dt} = -\frac{R_i}{L_i}Q_i + \frac{1}{L_i}(P_i - P_{i+1}) \tag{1}$$

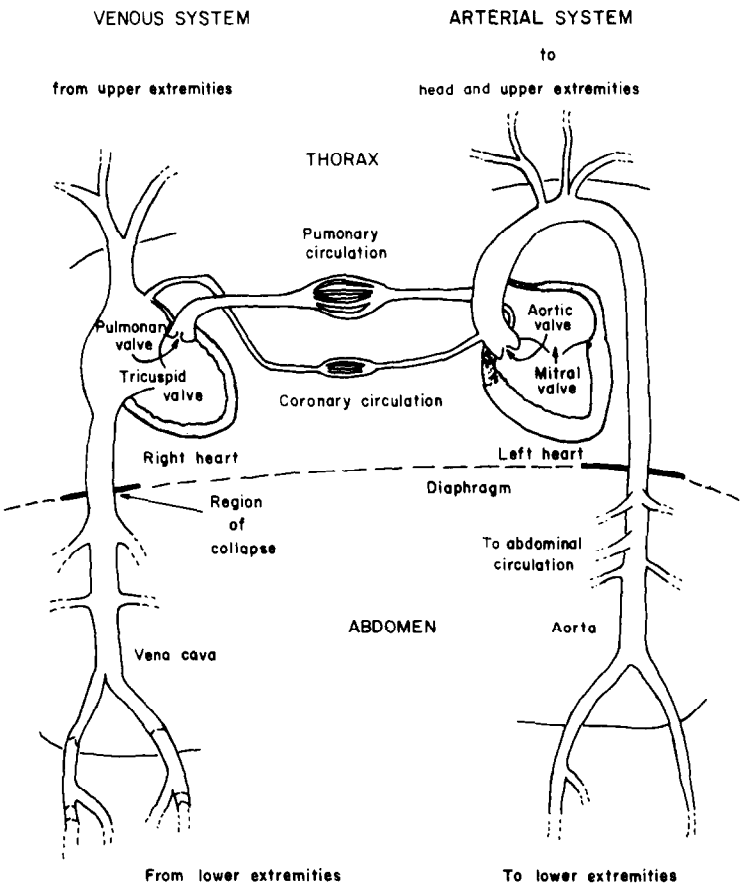

FIG. 1. Schematic presentation of the cardiovascular system.

$$\frac{dP_i}{dt} = \frac{Q_{i-1} - Q_i}{C_i}. \tag{2}$$

The cardiac chamber is assumed to have a negligible resistance and inductance values and is thus characterized solely by the capacitance. However, the heart chamber capacitance in the arrested, non-contracting, heart discussed here does not change with time. Consider a cardiac valve separating between any two capacitance chambers C_1 and C_2 in Fig. 2. The valve opens when P_1 is greater than P_2. The valve closes when the net flow Q across the valve is reversed, i.e. $Q \leqslant 0$, or

$$Q = \begin{cases} \dfrac{Q_1 C_2 + Q_2 C_1}{C_1 + C_2} & \text{open valve} \\ 0 & \text{closed valve.} \end{cases} \tag{3}$$

The existence of unidirectional valves in the venous system, distal to the outlets of the chest and abdomen, is a well-known physiological phenomenon. The effects of these valves in the related veins, are included here by assigning them resistance values which are much higher for the retrograde flow than for the antegrade flow. The value of the resistance to the retrograde flow correlates with the competence of the valve. A high resistance for retrograde flow represents a valve which is practically nonleaking.

A simple model of CPR

The above concepts have recently led Beyar *et al.* [20] to suggest the simple model of the cardiovascular system shown in Fig. 2. The chest and abdomen are included in a single integrated compartment and are simultaneously subjected to external pressure variations. The peripheral arteries and veins are exposed to a constant atmospheric pressure. The aortic valve (between the LV and the aorta) and tricuspid valve (between the right atrium and the right ventricle) are included in the model. The pulmonary and mitral valves are not included in the model, since ultrasonic measurements show that these valves are non-functional during CPR [5, 28, 29]. Table 1 summarizes the constants R, L, and C of the system which were taken from the literature (for a dog) [31, 32], or calculated from given geometrical data.

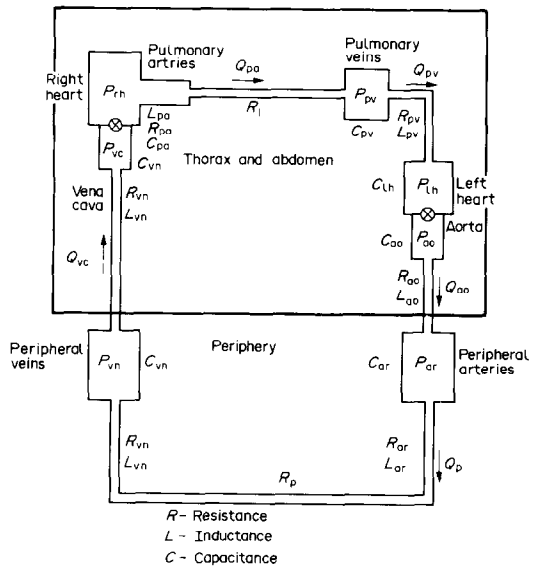

FIG. 2. A schematic outline of the basic CPR model. The thorax and abdomen (inner square) are exposed to pressure variations while the peripheral compartments head and extremities are subjected to atmospheric pressure.

Following Mashiro *et al.* [33], the pressure in the cardiovascular system in cardiac arrest was assumed to be equal in all the compartments. Square wave pressure pulses of different durations and amplitude were used to simulate the external compression pressures. Twelve differential equations, all of the first order, which characterize the system, are listed in the Appendix. The differential equations were solved in a single precision mode by the Runge–Kutta–Verner method [30] on an IBM 370 computer. The computations assuming pressure variation then proceeded, in steps of 0.01 s, until a steady state was achieved. Stabilization of the system was determined when the value of the volume displacement over one cycle was constant.

A typical set of calculated flow and pressure responses to the pressure pulse is given in Fig. 3. As seen in Fig. 3, a square thoracic pressure wave of 50 mm Hg generates an almost similar but somewhat higher pressure wave in the thoracic venous system (P_{vc}) than in the thorax, an overshoot in the aortic pressure (P_{ao}) and a smooth 'sinusoidal' arterial pressure wave (P_{ar}). The tricuspid valve is open throughout the cycle and the aortic valve opens during part of the compression period (artificial systole). The increase in the intrathoracic pressure is associated with forward flow (Q_{ao}) in the aorta and (due to the venous valves) only a minor retrograde flow (Q_{vc}) in the venous system. Releasing the intrathoracic pressure reverses the aortic flow, but the aortic valve closes and thus prevents the retrograde flow.

The calculated total net systemic flow throughout all the organs, at artificial systole and diastole durations ranging between 100 and 600 ms, ranges between 338 and 663 ml min^{-1}. These values are consistent with experimental measurements and are less than 25% of the baseline cardiac output of the dog. The effect of changing the duration of the high and low intrathoracic pressure periods, i.e. the artificial systole and artificial diastole, respectively, is presented in Fig. 4 as a three-dimensional plot of the cardiac output. A maximum cardiac output was obtained at a rate of 115 cycles per min and a duty cycle (the ratio of systole to total cycle time) of 0.58. This value is consistent with other reported results [34, 35].

The analysis of the above simple model shows that the intrathoracic pressure pulses generate blood flow in CPR, independent of direct heart compression between the thoracic bones. The magnitude of this flow is highly dependent on the efficiency of the venous and cardiac

Table 1. Parameter values for a typical 20 kg dog used in the two models

Simple model					Multicompartmental model			
Compartment	Symbol	R ((mm Hg) ml^{-1} min^{-1})	L (g cm^{-4})	C (ml (mm Hg)$^{-1}$)	Compartment	R ((mm Hg) ml^{-1} min^{-1})	L (g cm^{-4})	C (ml (mmHg)$^{-1}$)
Thoracic and abdominal arteries	ao	0.2	20	0.56	Thoracic aorta	0.1	15	0.2
					Abdominal arteries	0.1	5	0.25
Peripheral arteries	ar	0.55	3	0.61	Peripheral arteries	1.2	6	0.51
Peripheral resistance	R_p	2.04	—	—	Peripheral resistance	4	—	—
Peripheral veins	vn	0.15	0.3	26	Peripheral veins	0.31	0.6	22
					Great abdominal veins	0.03	0.5	15
Thoracic and abdominal veins	vc	0.06	2	22	Thoracic vena cava	0.03	1.5	7
					Coronoary circulation	10	1	—
					Intra-abdominal circulation	20	0.5	—
					External carotid arteries	0.5	3	0.05
					Intracranial arteries	0.5	3	0.05
					Brain circulation	7	0.1	—
					Intracranial veins	0.15	0.3	2
					External neck veins	0.15	0.3	2
Right heart	rh	—	—	4.6	Right heart	—	—	4.6
Pulmonary arteries	pa	0.175	0.625	1.5	Pulmonary arteries	0.175	0.625	1.5
Pulmonary resistance	R_l	0.325	—	—	Pulmonary resistance	0.325	—	—
Pulmonary veins	pv	0.1	0.3	3.5	Pulmonary veins	0.1	0.3	3.5
Left heart	lh	—	—	1.6	Left heart	—	—	1.6

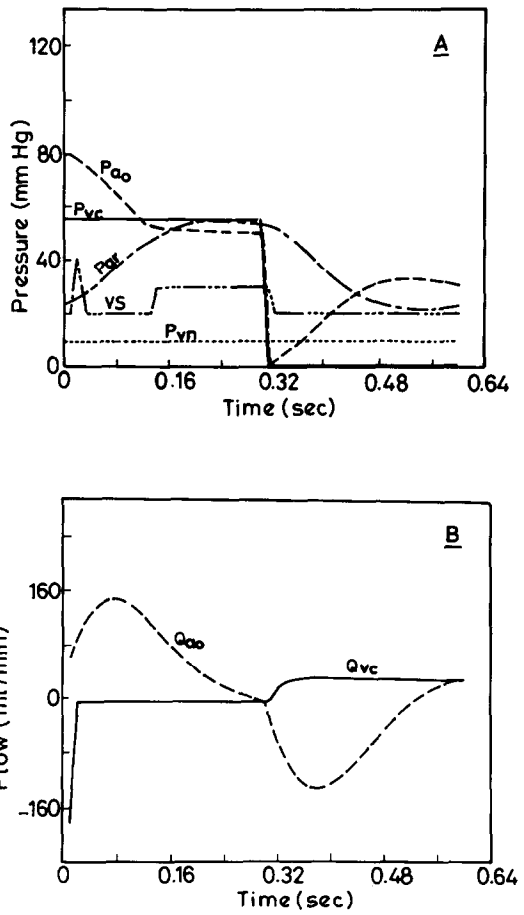

FIG. 3. Pressure and flow which develop in various compartments under a driving pressure of 50/0 mm Hg and a duty cycle of 50%. P, pressure; ao, aorta; vc, vena cava; ar, pheripheral arteries; vn, peripheral veins; vs, valve status. Note that vs = 40 represents closed aortic and tricuspid; vs = 30, aortic and tricuspid valves are open; vs = 20, the tricuspid valve is open and the aortic valve is closed. Q_{ao}, flow in the aorta; Q_{vc}, flow in the vena cava.

valves. The model predicts the optimal rate and duty cycle of CPR for a dog. However, the above model does not differentiate between the different organs, and does not provide details about regional blood flows in CPR. Furthermore, the thorax and abdomen are taken as a single compartment, subjected to equal pressures of a square wave type. These limitations can be overcome by utilizing the more sophisticated compartmental model presented here.

A multicompartmental model of the cardiovascular system during CPR

Consistent with reality, the model, schematically presented in Fig. 5, assumes that the thorax and abdomen chambers are independently subjected to different external pressures. The peripheral circulation (extremities, skin), the coronary flow, the intra-abdominal and head circulation are also included, separately, in the model. In addition to the aforementioned venous valves at the outlets of the chest and abdomen, a third valving mechanism, the 'Starling resistor mechanism' at the outlet of the vena cava at the neighborhood of the diaphragm, is included here.

Using Noordegraaf's [32] experimental data, the resistance R_{st} of the collapsible conduit is given by

$$R_{st} = 17.4R_0[P_{ab} - P_{th}] + R_0 \qquad (4)$$

where R_0 is the resistance of the segment without collapse, P_{ab} and P_{th} are the extravascular abdominal and thoracic pressures, respectively. It is evident that no collapse occurs at equal abdominal and thoracic pressures. The resistance increases when higher pressure driving forces ($P_{ab} - P_{th}$) are generated, and thus the flow in the collapsed segment remains relatively constant. The cardiovascular system presented in Fig. 5 is characterized by 30 differential equations, which are essentially similar to those presented in the Appendix. The external pressure waves

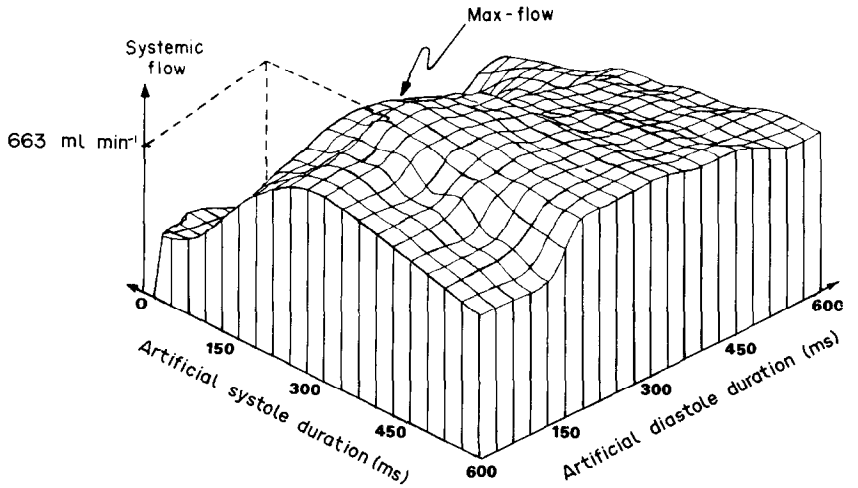

FIG. 4. A three-dimensional plot of the systemic blood flow vs artificial systole and diastole duration.

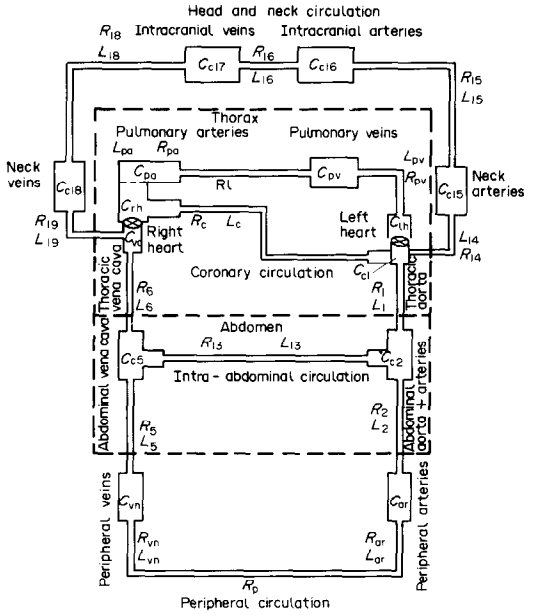

FIG. 5. A schematic illustration of the multicompartmental CPR model. Pressure variations can be independently simulated in the thorax and abdomen. Note that the coronary, head and neck and abdominal circulations are added.

on the chest and abdomen were assumed to have a sinusoidal shape. A more detailed description of the model is given elsewhere [21].

The results of the calculations highlight some important phenomena.

(a) The coronary blood flow occurs during the artificial diastole period and is reversed during artificial systole. These results have been confirmed experimentally [36], whereby the positive pressure driving force between the aorta and right atrium during the artificial diastole was found to enhance the coronary flow. Conversely, the small reversed pressure gradient during artificial systole was found to cause a small retrograde coronary flow.

(b) The pulmonary flow is maintained throughout the artificial systole and the artificial diastole. Increasing the intrathoracic pressure closes the venous valves, resulting in a positive flow from the intrathoracic cavities to the arterial system. As the intrathoracic pressure is released (artificial diastole), the pressure decreases in all the thoracic cavities. Closure of the aortic valve prevents the retrograde flow of arterial blood into the left ventricle. However, opening the venous valves allows the blood to flow from the relatively high pressure venous system (through the lungs) to the low pressure left ventricle. These results are in complete agreement with experimental data [37].

Table 2. Coronary flow (ml min^{-1}), in various pressure pulsing rates and different operating cycles

Pressure rate (cpm)	Duty cycle (ratio of artificial systole to cycle duration) 20%	30%	40%	50%	60%	70%
60	68.4	74.2	70.9	64.5	56.6	48.2
100	56.4	69.1	70.3	67.0	60.7	53.2
120	49.7	62.2	68.8	66.6	62.2	55.9

(c) Optimization of CPR pulsing rate and duration imposes a special problem. Table 2 gives the theoretical values of the coronary flow rate at different pulsing rates and different compression duty cycles. As is well known, the coronary flow occurs only during the artificial diastole period. Thus, systolic pressure periods, which are shorter than the 50% duty cycle needed for a maximum cardiac output, are suggested for a maximum coronary flow. Evidently, the presently recommended duty cycle of 50% (chest) compression during CPR does not yield the best coronary circulation and may have to be modified in the future.

(d) The introduction of a delay between the abdominal and the thoracic pressure waves has a significant positive effect on the cardiac output. A Starling resistor at the level of the diaphragm is assumed to be symmetrical and the resistance is thus proportional to the pressure difference between the chest and abdomen. Table 3 summarizes the effect of different delay times D (in ms) between the abdominal and thoracic pressure waves (with abdominal pressure preceding the thoracic pressure) on the cardiac output, carotid flow, coronary flow and pressure gradients. The cardiac output, carotid flow and coronary flow have maximum values at D = 300–400 ms and are followed

Table 3. The calculated effects of different phase lags between the abdominal and thoracic pressure waves on the hemodynamics in CPR

D (ms)	Cardiac output (ml min^{-1})	Carotid flow (ml min^{-1})	Coronary flow (ml min^{-1})	Peak aortic–right ventricular pressure gradient (mm Hg) Artificial systole	Artificial diastole
0	252	43.8	40.8	−6.4	26
150	365	58	62	−9	36
300	406	62	69	−11	40
400	395	61	67	−10	40

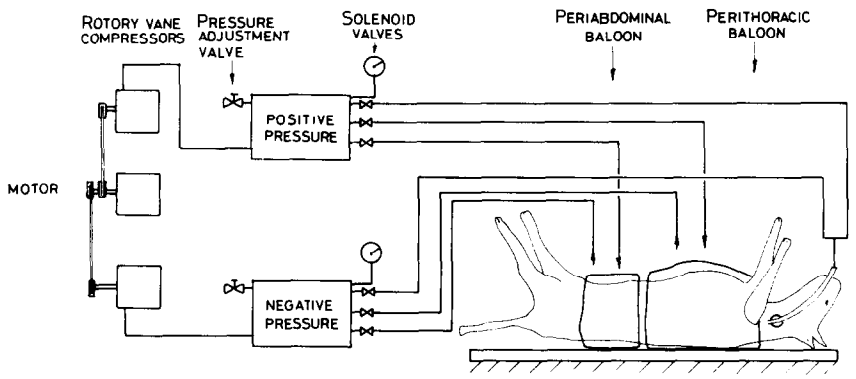

FIG. 6. Schematic presentation of the experimental cardiopulmonary resuscitation system with intrathoracic and abdominal pressure variation. The three compartments to be inflated and deflated are the lung, perithoracic bladder and periabdominal bladder.

by an increase in the diastolic pressure gradient between the aorta and the right ventricle.

ANIMAL STUDIES

The clinical animal studies, which complement the computer simulation had the following objectives: (a) confirm the theoretical finding that thoraco-abdominal pressure variations affect the systemic flow during CPR; (b) help understand the basic mechanisms involved in CPR by relating and comparing the *in vivo* experimental data to the results derived from the computer model; and (c) improve the current CPR technique.

The experimental set-up is schematically depicted in Fig. 6. Positive and negative pressure rotary vane compressors feed two reservoirs in which the pressure level can be adjusted by a valve. Three solenoid valves feed the three compartments with air from the positive pressure reservoir and three valves evacuate the air. The solenoid valves are controlled by a specially designed electronic controller.

Inflation and deflation rates of the three compartments—lung, chest and abdomen—could be independently controlled. The dog's heart was fibrillated by an intravenous injection of 1 g KCl. Pressure measurements were carried out in the aorta, and the left and right ventricles by using Millar Microtip manometers. Blood flow was measured in the carotid artery by an electromagnetic flowmeter. Table 4 gives typical values of the flows and pressures in the system. The right ventricular pressure exceeds the aortic pressure during artificial systole, and the pressure gradient reverses in artificial diastole. The experimental pressures and flow rates are compared in Fig. 7 with the computer results at similar conditions of external pressures and rates. As seen, the diastolic gradient is lower in the theoretical model than in the experiments. Although the agreement is not complete, the model results are a fair approximation of the experimental results. The pressure gradients are comparable. A biphasic cartotid flow wave is shown by both the mathematical and the experimental model.

The effects of the delay time between the thoracic and abdominal pressure waves in a phased compression cardiopulmonary resuscitation (PCCPR) was studied in six dogs, utilizing a cycle of 1000 ms. The delay time varied from 0 ms, i.e. simultaneous compression of chest and abdomen, to 400 ms between the abdominal balloon inflation and the subsequent thoracic balloon inflation. As seen in Table 5, increasing the delay between the thorax and abdomen pressure waves has a favorable effect on cardiac output as well as on the carotid flow. Similar qualitative results have recently been reported by Voorhees *et al.* [18]. It is noteworthy that although the coronary flow was not measured

Table 4. Measured pressures and flows during CPR. The rate of pressure pulses was 60 ÷ 100 cpm

Aortic pressure (mm Hg)		Right ventricular pressure (mm Hg)		Carotid flow	Carotid flow index*
Artificial systole	Artificial diastole	Artificial systole	Artificial diastole	(ml min^{-1})	
89.3 ± 20.5	17.5 ± 3.3	96.7 ± 20.5	11.7 ± 2.6	21.7 ± 7.8	0.18 ± 0.06

*The carotid flow index is the average CPR flow values divided by the average baseline flow values.

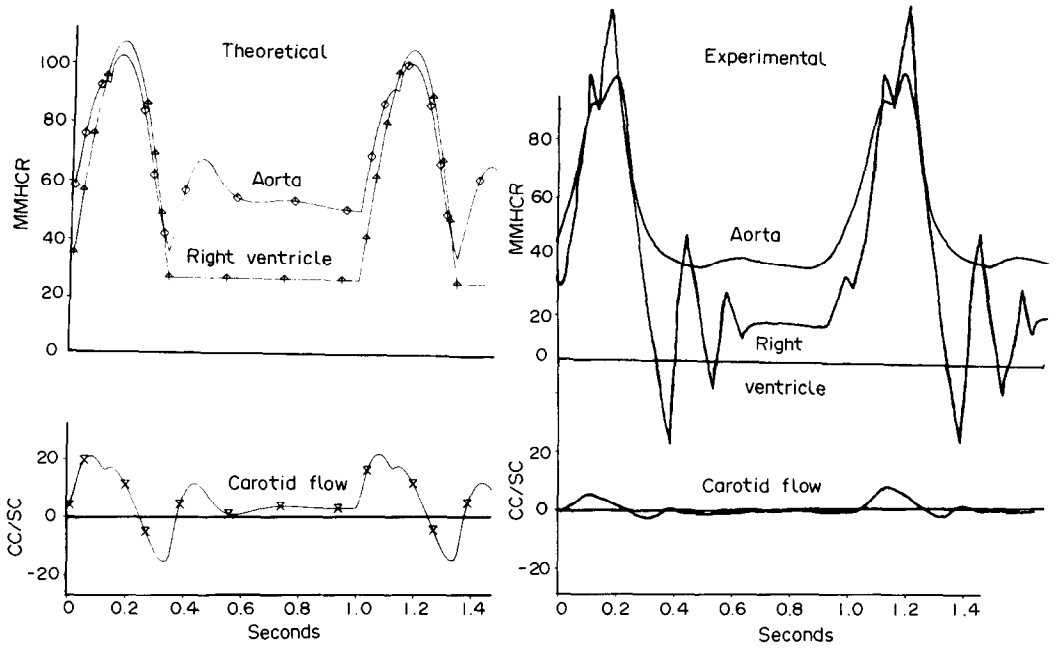

FIG. 7. A comparison between experimental *in vivo* pressures and carotid flows and the comparable computer results.

experimentally here, the mathematical model indicates a highly favorable effect of the PCCPR on this flow (Table 3).

Figure 8 shows the pressure in the thoracic and abdominal vena cava in two different CPR modes of operation. The measurements were done below and above the diaphragm—only a few centimeters apart. The observed peak pressure differences between the thoracic and abdominal vena cava are attributed to the collapse of a small segment of the vena cava near the diaphragm. Note that the collapse occurs when the abdomen is unrestrained and uncompressed and thus the abdominal pressure is much lower than the thoracic pressure. Essentially similar results are noted when the abdomen is compressed 300 ms before the thorax. Consistent with equation (4), no gradient was measured across the diaphragm where the abdomen and the thorax were compressed simultaneously.

CONCLUSIONS

The development of a new clinical technique for cardiopulmonary resuscitation, based on computer simulation models and clinical animal trials, is outlined. The analysis provides new insight into the blood flow phenomena during CPR and the analysis of the mathematical and experimental models clarifies the flow mechanisms involved in CPR during cardiac arrest.

In the classical CPR operation, whereby the chest is compressed by mechanical means ('the chest pump'), most of the pressure pulsations are imposed on the thorax. By collapsing near the diaphragm, the vena cava acts like a Starling resistor, while the venous valves distal to the outlet of the chest and the abdomen prevent retrograde flow. The chest pump mobilizes the pulmonary flow throughout the cycle and activates pulsatile systemic flow, systolic flow through the aortic valve and diastolic flow through the coronary vessels. Venous return (flow of venous blood into the chest) is restricted to the artificial diastole period. Finally, the model indicates that the maximum coronary flow in CPR occurs with shorter artificial systolic periods than those needed to obtain a maximum cardiac output.

CPR by simultaneous thoracic and abdominal compression is characterized by an almost even

Table 5. The effect of thoracic-abdominal phase lag on the cardiac output and carotid flow in the dogs

Mode	$D = 0$ ms	$D = 150$ ms	$D = 300$ ms	$D = 400$ ms
Carotid flow index*	0.13 ± 0.076	0.146 ± 0.105	0.22 ± 0.12	0.24 ± 0.12
Cardiac output index*	0.073 ± 0.03	—	0.126 ± 0.03	—

D, Time delay between the abdominal and thoracic pressure waves.
* The ratio of the CPR flow to normal flow before the cardiac arrest.

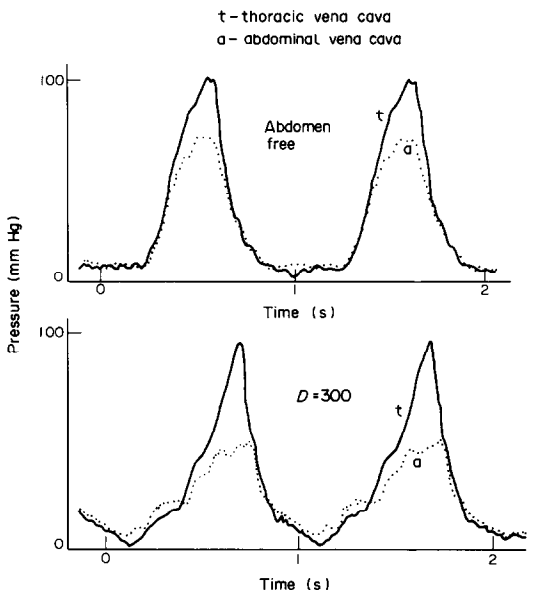

FIG. 8. Measured pressures in the thoracic vena cava and abdominal vena cava during two modes of CPR operation.

increase in the abdominal and thoracic pressures, which minimizes the collapse of the vena cava at the neighborhood of the diaphragm. Thus, the peripheral venous valves play a larger role in preventing the retrograde flow than in the abdomen-free situation of the classical CPR. The improved cardiac output obtained here is due to the increased pressure amplitudes in this procedure as compared with the classical CPR under the same pressure driving force.

In the PCCPR, the newly suggested sequential thoraco-abdominal pumping technique, the abdominal pressure mobilizes the venous blood from the abdomen to the chest. The subsequent thoracic pressure wave pushes the blood within the chest to the peripheral arterial system. Thus, the combined effect of the sequential abdomen and chest compressions is to generate higher blood flows to the vital organs, thus improving chances of survival from cardiac arrest.

The suggested PCCPR procedure of a sequential thoraco-abdominal pump may develop into a tool of clinical importance in cardiac arrest cases and as a cardiac assist device in cases of cardiogenic shock. The study represents an excellent example of the advantage of the interaction between the theoretical analysis of blood flow phenomena under extreme conditions and an important practical medical problem.

Acknowledgements—This study was supported by the U.S.-Israel Bi-national Foundation and the Kennedy Leigh Fund, London. We are grateful to both for their trust and encouragement. The help and support of the Heart Center, Sheba Medical Center is highly appreciated.

REFERENCES

1. G. J. MacKenzie, S. H. Taylor, A. H. McDonald and K. W. Donald, Hemodynamic effects of external cardiac compression, *Lancet* **1**, 1342 (1964).
2. W. B. Kouwenhoven, J. R. Jude and G. G. Knickerbocker, Closed chest cardiac massage, *JAMA* **173**, 1064 (1960).
3. W. B. Kouwenhoven, J. R. Jude and G. G. Knickerbocker, Closed chest cardiac massage, *Lancet* **1**, 990 (1962).
4. J. T. Niewmann, J. Rosborough, M. Hausknecht, D. Brown and M. Criley, Cough CPR, *Crit. Care Med.* **8**, 141 (1980).
5. J. A. Werner, L. Greene, C. L. Janko and L. A. Cobb, Visualization of cardiac valve motion in man during external chest compression using two-dimensional echocardiography, *Circulation* **63**, 1417–1421 (1981).
6. M. T. Rudikoff, W. L. Maughan, M. Efforn, P. Freund and M. L. Weisfeldt, Mechanisms of blood flow during cardiopulmonary resuscitation, *Circulation* **61**, 345–353 (1980).
7. N. Chandra, R. M. Rudikoff, J. Tsitlik and M. L. Weisfeldt, Augmentation of carotid flow during CPR in the dog by a simultaneous compression and ventilation with high airway pressure, *Am. J. Cardiol.* **43**, 422 (1979).
8. N. Chandra, M. Rudikoff and M. Weisfeldt, Simultaneous chest compression and ventilation at high airway pressure, *Lancet* **1**, 175–178 (1980).
9. N. Chandra, M. Weisfeldt, J. Tsitlik, F. Vaghaiwalla, L. D. Snyder, M. Hoffecker and M. Rudikoff, Augmentation of carotid flow during cardiopulmonary resuscitation by ventilation at high airway pressure simultaneous with chest compression, *Am. J. Cardiol.* **48**, 1053 (1981).
10. C. F. Babbs, W. A. Tucker, R. L. Paris, K. J. Murphy and R. W. Davis, Cardiopulmonary resuscitation with simultaneous compression and ventilation at high airway pressure for animal models, 4th Purdue Conf. on Cardiac Defibrillation and Cardiopulmonary Resuscitation, 15–17 September (1981).
11. N. Chandra, L. D. Snyder and M. L. Weisfeldt, Abdominal binding during CPR in man, *JAMA* **246**, 351 (1981).
12. J. P. Rosborough, J. T. Niemann, J. M. Criley, W. O'Bannon and D. Rouse, Lower abdominal compression with synchronized ventilation: a CPR modality (abstr.), *Circulation* **64** (Suppl. IV), 303 (1981).
13. R. C. Koehler, N. Chandra, A. D. Guerci, J. Tsitlik, R. J. Traystman, M. C. Rogers and M. L. Weisfeldt, Augmentation of cerebral perfusion by simultaneous chest compression and lung inflation with abdominal binding after cardiac arrest in dogs, *Circulation* **67**, 266 (1983).
14. W. D. Voorhees, C. F. Babbs and W. A. Tacker, Jr., Regional blood flow during cardiopulmonary resuscitation in dogs, *Crit. Care Med.* **8**, 134 (1980).
15. J. M. Luce, B. K. Ross, R. J. O'Quin, B. H. Culver, M. Sivarajan, D. W. Amery, R. A. Niskanen, C. A. Alferness and W. L. Kirk, Regional blood flow during cardiopulmonary resuscitation in dogs using simultaneous and nonsimultaneous compression and ventilation, *Circulation* **67**, 258–265 (1983).
16. M. Weisfeldt, J. E. Tsitlik, A. D. Guerci, H. R. Halperin and H. R. Levin, The effects of high doses of adrenaline in CPR, Personal communication (1983).
17. E. Kimmel, R. Beyar, U. Dinnar, S. Sideman and Y. Kishon, Cardiopulmonary resuscitation by chest and abdomen phased compression Technion R & D Report No. 130–108/112 (1983).
18. W. D. Voorhees, M. J. Niebaur and C. F. Babbs, Improved oxygen delivery during CPR with manual abdominal counter thoracic abdominal pulsation, *Circulation* **66** (Suppl. II), 168 (1982).
19. R. Beyar, Y. Kishon and U. Dinnar, Cardiopulmonary resuscitation mechanisms: a computer model, *Biomed. Eng. Trans. Proc. of the 5th Ann. Conf. Front. Eng. Comp. Health Care*, Columbus, Ohio, U.S.A. (1983).
20. R. Beyar, Y. Kishon, U. Dinnar and H. Neufeld, Cardiopulmonary resuscitation by intrathoracic pressure variation—computer simulation and *in vivo* studies, *Angiology* **34**, 71–78 (1984).

21. R. Beyar, Y. Kishon, S. Sideman and U. Dinnar, Computer studies of systemic and regional blood flow mechanisms during cardiopulmonary resuscitation, *Med. Biol. Eng. Comp.*, in press.
22. R. Beyar and U. Dinnar, Computer simulation of cardiopulmonary resuscitation, *J. Biomed. Engng*, in press.
23. J. E. W. Beneken, A mathematical approach to the cardiovascular function. The uncontrolled human system, Int. Rep. 2.4.5/6, Inst. of Medical Physics TNO Uterecht (1965).
24. J. E. W. Beneken, Some computer models in cardiovascular research, in *Cardiovascular Fluid Dynamics* (edited by D. H. Bergel), p. 173. Academic Press, New York (1972).
25. O. Frank, Die Grundform des arteriellen pulses, *Z. Biol.* **37**, 483 (1899).
26. V. C. Rideout, Cardiovascular system simulation in biomedical engineering education, *IEEE Trans. BME* **19**, 101 (1972).
27. O. Frank, Schatzung des Schlagvolumes des menschlikhen herzen auf grund der wellen und windkesselstheorie, *Z. Biol.* (Munich) **90**, 405 (1930).
28. S. Rich, H. L. Wix and E. Shapiro, Two dimensional echocardiograph of the heart during cardiopulmonary resuscitation in man, *Am. J. Cardiol.* **47**, 398 (1981).
29. S. Rich, H. L. Wix and E. P. Shapiro, Clinical assessment of heart chamber size and valve motion during cardiopulmonary resuscitation by two-dimensional echocardiography, *Am. Heart J.* **102**, 368 (1981).
30. B. Cornahan, N. A. Luther and J. O. Wilkes, *Applied Numerical Methods*, p. 361. Wiley, New York (1969).
31. P. L. Altman and D. S. Dittmer, *Respiration and Circulation*, p. 359. Federation of American Societies for Experimental Biology, Bethesda, Maryland (1972).
32. A. Noordegraaf, *Circulatory System Dynamics*, Vol 1, pp. 185, 286. Academic Press, New York (1978).
33. I. Mashiro, J. N. Cohn, R. Heckel, R. R. Nelson and J. A. Franciosa, Left and right ventricular dimensions during ventricular fibrillation in the dog, *Am. J. Physiol.* **235**, 231 (1978).
34. G. J. Taylor, W. M. Tucker, H. L. Greene, M. T. Rudikoff and M. W. Weisfeldt, Importance of prolonged compression during cardiopulmonary resuscitation in man, *NEJM* **296**, 1515 (1977).
35. C.F. Babbs, K. R. Fitzgerald, D. I. Silver, H. A. Frissora and L. A. Geddes, Influence of compression duration and compression rate upon cardiac output during CPR in dogs, *Crit. Care Med.* **8**, 248 (1980).
36. R. F. Bellamy, L. R. DeGuzman and D. C. Peders, Coronary flow during cardiopulmonary resuscitation in swine, *Circulation* **68** (Suppl. III), 236 (1983).
37. J. M. Cohen, N. Chandra, P. O. Alderson, A. V. Aswegen, J. E. Tsitlik and M. L. Weisfeldt, Timing of pulmonary and systemic blood flow during intermittent high intrathoracic pressure cardiopulmonary resuscitation in the dog, *Am. J. Cardiol.* **49**, 1883 (1982).

APPENDIX

The simple model illustrated in Fig. 2 is represented by a set of 12 differential equations listed below

$$\frac{dQ_{ao}}{dt} = -\frac{R_{ao}}{L_{ao}}Q_{ao} + \frac{P_{lh} - P_{ar}}{L_{ao}} \tag{A1}$$

$$\frac{dQ_{p}}{dt} = -\frac{R_{p} + R_{ar} + R_{vn}}{L_{ar} + L_{vn}}Q_{p} + \frac{P_{ar} - P_{vn}}{L_{ar} + L_{vn}} \tag{A2}$$

$$\frac{dQ_{vc}}{dt} = -\frac{R_{vc}}{L_{vc}}Q_{vc} + \frac{P_{vn} - P_{vc}}{L_{vc}} \tag{A3}$$

$$\frac{dQ_{pa}}{dt} = -\frac{R_{l} + R_{pa}}{L_{pa}} + \frac{P_{rh} - P_{pv}}{L_{pa}} \tag{A4}$$

$$\frac{dQ_{pv}}{dt} = -\frac{R_{pv}}{L_{pv}}Q_{pv} + \frac{P_{pv} - L_{lh}}{L_{pv}} \tag{A5}$$

open aortic valve:
$$\frac{dP_{ao}}{dt} = \frac{Q_{pv} - Q_{ao}}{C_{lh} + C_{ao}} \tag{A6}$$
$$\frac{dP_{lh}}{dt} = \frac{Q_{pv} - Q_{ao}}{C_{lh} + C_{ao}} \tag{A7}$$

closed aortic valve:
$$\frac{dP_{ao}}{dt} = -\frac{Q_{ao}}{C_{ao}} \tag{A6}$$
$$\frac{dP_{lh}}{dt} = -\frac{Q_{pv}}{C_{lh}} \tag{A7}$$

$$\frac{dP_{ar}}{dt} = \frac{Q_{ao} - Q_{p}}{C_{ar}} \tag{A8}$$

$$\frac{dP_{vn}}{dt} = \frac{Q_{p} - Q_{vc}}{C_{vn}} \tag{A9}$$

open tricuspid valve:
$$\frac{dP_{vc}}{dt} = \frac{Q_{vc} - Q_{pa}}{C_{vc} + C_{rh} + C_{pa}} \tag{A10}$$
$$\frac{dP_{rh}}{dt} = \frac{Q_{vc} - Q_{pa}}{C_{vc} + C_{rh} + C_{pa}} \tag{A11}$$

closed tricuspid valve:
$$\frac{dP_{vc}}{dt} = \frac{Q_{vc}}{C_{vc}} \tag{A10}$$
$$\frac{dP_{rh}}{dt} = -\frac{Q_{pa}}{C_{rh} + C_{pa}} \tag{A11}$$

$$\frac{dP_{pv}}{dt} = \frac{Q_{pa} - Q_{pv}}{C_{pv}}. \tag{A12}$$

Four combinations of arotic and tricuspid valve positions are possible. The detailed model which is represented in Fig. 5 is described by a set of 30 differential equations derived for each compartment as for the simple model.

EFFET DE L'ONDE DE PRESSION THORACIQUE ET ABDOMINALE SUR L'ECOULEMENT DU SANG EN REANIMATION CARDIOPULMONAIRE

Résumé—Fondés sur l'hypothèse des variations de pression induites dans la cage thoracique pour recréer la circulation du sang pendant la réanimation cardiopulmonaire (CPR) après un arrêt cardiaque, des modèles mathématiques de complexité croissante sont développés pour décrire le phénomène de circulation dans un système cardiovasculaire. La représentation par paramètre centré du système cardiovasculaire décrit le phénomène d'écoulement pendant la CPR et permet l'optimisation de la technique CPR et suggère aussi une nouvelle procédure CPR. Des études cliniques expérimentales (chiens) confirment la prévision selon laquelle une compression abdomino-thoracique séquentielle (PCCPR) cause des écoulements du sang qui sont deux fois les valeurs obtenues dans le mode classique CPR par compression manuelle de la cage thoracique. La nouvelle technique PCCPR proposée accroit fortement l'irrigation des organes vitaux et elle ouvre une nouvelle direction dans le domaine de la médecine d'urgence.

DER EINFLUSS VON THORAX- UND BAUCHDRUCKWELLEN AUF DIE BLUTSTRÖMUNG BEI DER HERZ-LUNGEN-WIEDERBELEBUNG

Zusammenfassung—Ausgehend von der Annahme, daß äußerlich herbeigeführte Druckänderungen in der Brusthöhle einen lebenserhaltenden Blutstrom während der Herz-Lungen-Wiederbelebung (HLW) bei Herzstillstand erzeugen, wurden mathematische Modelle von zunehmender Komplexität zur Beschreibung der Strömung im Herzkranzgefäßsystem entwickelt. Die mathematische Modellierung des Herzkranzgefäßsystems mittels konzentrierter Parameter gestattet, die Strömungsphänomene während der HLW zu beschreiben und läßt sich sowohl zur Optimierung der gegenwärtigen HLW-Technik als auch zur Entwicklung eines neuen HLW-Verfahrens verwenden. Klinische experimentelle Untersuchungen (Hunde) bestätigen die Voraussage, daß eine aufeinanderfolgende Bauch-Thorax Kompression (PCCPR) zu Blutströmungen führt, welche zweimal so groß sind wie die Werte, die mit der klassischen HLW-Methode der manuellen Brustkompression erhalten werden. Die kürzlich vorgeschlagene PCCPR-Technik verbessert erheblich den Blutstrom durch lebenswichtige Organe bei der HLW und ist richtungsweisend auf dem Gebiet der Notfallmedizin.

ВЛИЯНИЕ ВОЛН ДАВЛЕНИЯ В ГРУДНОЙ И БРЮШНОЙ ПОЛОСТЯХ НА КРОВОТОК ПРИ ВОССТАНОВЛЕНИИ СЕРДЕЧНО-ЛЕГОЧНОЙ ФУНКЦИИ

Аннотация—По гипотезе авторов индуцированные внешними воздействиями изменения давления внутри грудной полости вызывают при остановке сердца жизненно важный ток крови, содействующий восстановлению сердечно-легочной функции (ВСЛФ). На этой предпосылке основываются сложные математические модели для описания картин течения в сердечно-сосудистой системе. Кусочно-параметрическое представление сердечно-сосудистой системы позволяет охарактеризовать течение при ВСЛФ, оптимизировать существующую и предложить новую методику ВСЛФ. Клинические опыты (на собаках) подтверждают теоретический вывод, что последовательно фазированное сжатие брюшной и грудной полостей создает кровоток в 2 раза более интенсивный, нежели при классическом ручном способе надавливания на грудную клетку. Предлагаемый метод значительно улучшает кровоснабжение жизненно важных органов при ВСЛФ и открывает новые возможности для экстренной терапии.